USING TIME OF FLIGHT DISTANCE CALCULATIONS FOR TAGGED SHARK LOCALIZATION WITH AN AUV

Yukun Lin, Hannah Kastein
Taylor Peterson, Christopher Clark
Harvey Mudd College
Claremont, California 91711
{ylin, hkastein, tpeterson, clark}
@hmc.edu

Connor White, Christopher Lowe
Department of Biological Sciences
CSU Long Beach
Long Beach, CA 90840
connor.white@student.csulb.edu,
clowe@csulb.edu

***Abstract*---Tracking fish has primarily been accomplished using acoustic telemetry. Typically, a fish is tagged, released, and manually tracked using hydrophones that detect acoustic tag transmissions. More recently, such hydrophone receiver systems have been mounted on Autonomous Underwater Vehicles (AUVs) to increase system mobility. This paper presents a new method for determining the distance from a tag to an AUV equipped with such a hydrophone system. By first estimating the transmission time of a tag signal, the time-of-flight can be used to calculate the distance to a tag. Furthermore, the calculated distance can be incorporated into an online state estimator to more accurately localize a tagged target. Results indicate significant improvement in an AUV's ability to localize a target when the distance to tag calculations are used in combination with angle-to-tag measurements.**

I. Introduction

Motion behavior study of sharks and other fish is an important tool for monitoring and maintaining fish populations and their habitat. Typical methods for tracking fish and sharks include tagging individuals with acoustic transmitters, and then using hydrophone receiver systems that detect and measure the signals transmitted. Often, the hydrophone receivers are placed at static locations around an environment of interest [1]. Alternatively, active tracking can be done manually by mounting a directional hydrophone on a boat and following the tagged individual for up to 96 hours [2].

To enable active tracking without the need for human operators, the authors have demonstrated that Autonomous Underwater Vehicles (AUVs), equipped with a stereo-hydrophone system that provides angle-to-tag measurements, are able to autonomously track and follow tagged leopard sharks [3]. Key developments by Forney et al. included a particle filter shark state estimator that could accommodate the low-resolution, low-sampling frequency and the sign ambiguity associated with angle measurements of the stereo-hydrophone system [4].

The work presented in this paper builds on previous work by incorporating a new method for obtaining distance-to-tag measurements using time-of-flight calculations. When fused with angle-to-tag measurements within the state estimator, tag localization accuracy is improved.

What follows below is a brief review of related work in Section II, followed by a description of the problem being addressed in Section III. In Section IV, the proposed approach to shark state estimation that incorporates distance-to-tag measurements is presented. Section V presents experiments and results that validate the use of the new measurements, followed by conclusions in Section VI.

II. Background

Tracking stationary and moving targets with robotic systems is a well-studied field of research ([5]--[10]). Within the context of using underwater robots to track individuals, both optical based methods ([11]--[13]), and acoustic based methods ([14], [15]) have been used. In Rife et al., autonomous tracking of jelly fish with an ROV

was conducted using basic image processing techniques [11]. Work presented in Zhou et al. demonstrated the use of SIFT features in tracking individual fish between video frames captured from an ROV [12]. Image processing techniques were also shown to be useful in tracking divers with a robot in Georgiades et al. [13]. Unfortunately, most optical methods employed in the underwater environment suffer from limited visibility due to poor lighting conditions and the presence of debris.

While acoustic methods of tracking marine individuals have been used for decades, hydrophone receivers have only recently been mounted on underwater vehicles. For example, work done by Grothues et al. has demonstrated the ability to track tagged sturgeon using a REMUS AUV equipped with a Lotek hydrophone system ([10], [14], [16]). Unlike the work presented by the authors, work by Grothues et al. did not use distance calculations nor in-situ measurements to actively steer the AUV ([10], [14], [16]).

The method of incorporating time-of-flight calculations to aid in localization in underwater robotics is not novel. Systems of static receiver arrays on the ocean floor have used the different time of detection of neighboring hydrophones to triangulate the position of a tagged target [1]. In Kussat et al., the two way travel times between an AUV and fixed transponders on ocean floor, aided by GPS measurements, were used to localize the AUV with high precision [17]. The method described in this paper, however, uses only the predicted one way travel time from transmitter to receiver to calculate distance.

Another method to obtain distance-to-tag measurements is by determining the relationship between received signal strength and distance a priori, before using this relationship in-situ. While there exists a negative correlation between distance and signal strength, the relationship is non-linear and highly dependent on environmental variables [3]. Hence, extracting distance measurements using this relationship often leads to high localization errors.

One problem that is encountered during state estimation is the low and unpredictable frequency of good measurements from the hydrophones. To address similar issues, Monte Carlo Localization (MCL) methods have been used in the past ([4], [18]--[22]). Unfortunately, lack of good measurements can lead to particle deprivation. Works that include improved variants of MCL to handle particle deprivation include Hwang et al. and Thrun et al. ([23], [24]). In Hwang et al., a genetic filter that uses residual mutation to ”push” lost particles towards the target is presented [23]. Thrun et al. presents augmented Monte Carlo Localization (aMCL), which adds random particles based on the long- and short-term likelihoods of sensor measurements to prevent clustering of particles in wrong locations [24].

The work presented below improves on existing AUV based acoustic tag tracking by incorporating time-of-flight distance calculations into a state estimator to improve target tracking accuracy.

III. Problem Overview

The goal of this work is to estimate the 2D position of a tagged shark using an AUV equipped with a stereo-hydrophone system. Details of both the hardware system and state estimation problem are described below.

A. Hardware System

The system consists of two OceanServer Iver2 AUVs. The Iver2 AUV is a torpedo-shaped robot (see Fig. 1), that has a rear propeller to provide locomotion, and four fins to control the vehicle’s pitch and yaw. The sensor payload includes a 3-DOF compass, wireless antenna, GPS receiver, and Doppler Velocity Logger. The AUVs communicate with each other, as well as with a topside modem, via a Woods Hole Oceanographic Institution Micro-Modem and externally mounted transducers. Each AUV is outfitted with a Lotek MAP600RT receiver and an associated stereo-hydrophone set, designed to listen for acoustic signals at a frequency of 76 kHz. These allow the vehicles to receive transmissions from Lotek MM-M-16-50-PM acoustic tags (see Fig. 2), which transmit at 76.8 kHz. The Lotek MapHost software associated with the receiver records the tag ID, time of detection, signal strength, pressure, and presence of motion.

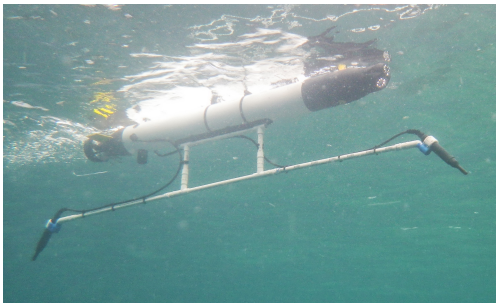

Fig. 1: Hydrophones mounted on a prototype PVC frame attached to an OceanServer Iver2, suspended 0.4 meters down with 2.4 meters of separation.

The two hydrophones of the stereo-hydrophone system are mounted 2.4 meters apart and suspended 0.4 meters beneath each AUV. The separation of the hydrophones, shown in Fig. 1, allows the angle between the AUV and the acoustic tag to be calculated.

Fig. 2: Lotek MM-M-16-50-PM acoustic tag.

Every two seconds, the tag sends a burst of three transmissions, called codes. Each code is identified by a numerical ID. Depending on the tag, the three codes are chosen from either five or six possible different codes, each with different IDs. The Lotek receiver software is capable of recording the time of reception of each code with a resolution of 10^{-5} seconds.

B. State Estimation Problem

The state of the AUV and sensor measurements at time t are denoted by $X_{auv,t}$ and Z_t, respectively. The hydrophones are mounted on the nose and tail ends of the AUV; the difference in time of arrival of a tag transmission is used by the Lotek receiver software to calculate the angle to the shark, denoted by z_α. Using the time of arrival measurement z_{toa}, the distance-to-tag can be obtained. The state estimator uses

$$X_{auv,t} = [x_{auv}\ y_{auv}\ \theta_{auv}]_t \tag{1}$$

and

$$Z_t = [z_{toa}\ z_\alpha]_t \tag{2}$$

to calculate the estimated shark state

$$X_{shark,t} = [x_{shark}\ y_{shark}\ \theta_{shark}\ v_{shark}]_t. \tag{3}$$

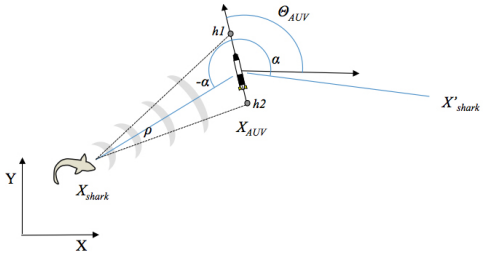

Fig. 3: An overview of the shark state estimation problem.

There are several challenges associated with state estimation given the sensor measurements. As illustrated in Fig. 3, a shark located at X_{shark} will generate the same angle measurement as a shark located at X'_{shark}. In addition, the stereo-hydrophone system generates an angle-to-tag measurement with a low resolution of approximately 10 degrees. Furthermore, the rate at which an angle measurement is obtained is highly dependent on the acoustic environment; time intervals of up to 30 seconds were observed in which no angle measurements were obtained. Even with distance measurements, the shark state $X_{shark,\,t}$ cannot be determined solely using geometry. To address this issue, MCL methods are used by the state estimator.

IV. State Estimation Methodology

A. Overview

The steps required for online state estimation using time-of-flight distance measurements are described in the following section. First, before the

tag and AUV are deployed, an offline calibration is required that enables determination of two constants associated with any tag code: the period of transmission T_c and the known initial transmission time t_0.

After offline calibration, the AUV and tag can be deployed for active tracking and online state estimation. Using the two constants T_c and t_0, along with the real-time signal time of arrival measurement z_{toa}, the time-of-flight for each tag transmission can be predicted and used to calculate the distance d to the tag. This distance, as well as the angle-to-tag measurement z_α, is used to estimate the shark state X_{shark} in real time.

B. Offline Calibration

1) Transmission Period Calibration: Before the AUV and tag can be deployed, the period of the tag transmission, T_c, is determined by calculating the mean difference in the consecutive time-of-arrival measurements z_{toa} when the tag is located adjacent to the hydrophone. The acoustic tags transmit each code with a precise period, allowing an accurate prediction of the time of transmission for each code. Codes for different tags will transmit with either two second or four second periods. Table I provides example transmission period data that was obtained by taping an acoustic tag to the hydrophones in air, and recording the times of detection of the tag codes for roughly 100 minutes.

Time Difference [s]	Frequency
0.04875	3
0.04896	1
3.95104	3
3.99958	55
3.99959	30
3.99979	1172
3.99980	235
3.99999	1
4.00000	43
7.95063	1
7.99937	1
7.99958	1

TABLE I: The frequencies of time differences between consecutive transmissions of the tag code 117 from Tag 55436 during a time set of 105 minutes.

2) Outlier Removal: As shown in Table I, there are several outlier time differences, due to problems such as missed signal detections. Hence, before the average transmission period T_c is calculated, the time differences between consecutive transmissions of a code are considered to be outliers when $|z_{toa,t} - z_{toa,t-1} - 4.00| > \tau$. In this work, τ = 0.01. For codes that transmit at roughly 0.5 Hz, transmissions are classified as outliers when $|z_{toa,t} - z_{toa,t-1} - 2.00| > \tau$.

After removing the defined outliers, the T_c is calculated by averaging the time differences. Time period values of the tags used are shown in Table II.

Tag ID	T_c [s]	σ Error [s]
55436	3.99979	0.00006
55488	1.99988	0.00010

TABLE II: Overview of transmission periods of code 117 for the two tags used. Code 117 was chosen because of its transmission frequency of 0.5 Hz for Tag 55488.

3) Initial Transmission Time Calibration: To determine a transmission time t_0 corresponding to the first tag signal broadcasted, the tag is placed adjacent to the hydrophones, and it is assumed that the first measured time of arrival is equal to the first transmission time, i.e. t_0 is set to be $z_{toa,t=0}$.

While the code transmission period T_c remains consistent even after the tag is power cycled, t_0 must be recalibrated each time the tag is turned back on. Power cycling the AUV also causes a time shift in the Lotek receiver's internal clock thereby requiring t_0 to be recalibrated.

If recalibration of t_0 is required, and the tag can be located at a known measured distance d_m, the initial transmission time can be corrected using Eq. 4.

$$t_{0,corrected} = t_{0,uncorrected} + \frac{d - d_m}{v} \qquad (4)$$

The term d in Eq. 4 is the uncorrected distance of the tag calculated at the same time step that d_m was measured.

If the tag is accessible and can be held directly next to the AUV, then the term $d_m = 0$. If

the tag cannot be measured directly, d_m can be approximated by the Euclidean distance between the estimated coordinates of the tagged target and the GPS coordinates of the AUV.

C. Online State Estimation

Once calibration is completed, real-time estimation is possible. At each time step of the AUV controller, the distance d to the tag is calculated first. The distance d and the angle-to-tag calculated by the Lotek receiver software are then used by the state estimator to localize the tag.

1) Calculating Distance: Given t_0, z_{toa}, and T_c, the distance of the tag to the hydrophone can be calculated as follows. The time $t_{transmit}$ is estimated by first determining the integer number of signal transmissions k for a code c that have occurred since t_0. The integer k is then calculated by Eq. 5.

$$k = \text{Round}\left[\frac{z_{toa} - t_0}{T_c}\right] \tag{5}$$

Thus, the estimated transmit time of the signal can be determined using Eq. 6.

$$t_{transmit} = t_0 + kT_c \tag{6}$$

The time-of-flight of the signal is $(z_{toa} - t_{transmit})$. Therefore, the distance d of the tag to the hydrophone is given by Eq. 7.

$$d = (z_{toa} - t_{transmit})v \tag{7}$$

It is important to note that the above calculations assume that there is no aliasing and that $z_{toa} - t_{transmit} < T_c/2$. For Eqs. 5- 7 to be valid, the maximum distance a tag can be located from the AUV is $vT_c/2$.

In the context of active tracking, the maximum threshold distance of $vT_c/2 \approx 1500\,\text{m}$ assuming $T_c \approx 2\,\text{s}$ is a feasible limitation. The AUV will ideally be following the tagged individual at a close distance. Depending on the acoustic environment, the maximum threshold distance likely will exceed the hydrophone's detection range.

Algorithm 1 Rejection of potential outliers in time-of-flight distance.

```
global d_previous
d_current ← time-of-flight distance
Δd ← |d_previous − d_current|
d_previous ← d_current
if Δd > Δd_max then
    return failed measurement
else
    return d_current
end if
```

2) Outlier Rejection: Similar to the offline calibration step, time difference outliers may occur during online distance calculations. To accommodate such outliers, Alg. 1 presents a simple online method for discarding potential outliers.

In the implementation that follows, a conservative value of $\Delta d_{max} = 50\,\text{m}$ is chosen. Given most tagged individuals will not be traveling at velocities greater than $4\,\text{ms}^{-1}$, their greatest distance travelled during a single transmission period of $4\,\text{m}$ would at worst result in $16\,\text{m}$ distance travelled. It is highly unlikely that a change in distance between the tag and the AUV greater than $50\,\text{m}$ would occur during the time spanned between two measurements.

3) Augmented MCL: The online state estimator uses aMCL to estimate the position of the tagged target. The belief of the tagged target's location at time t is represented by a set of particles P_t, where the i^{th} particle $p_i \in P_t$ is defined by its shark state $X_{shark,t}$ as in Eq. 1 as well as by a weight w_i that indicates the likelihood that p_i is the true state. Initially, particle states are assigned a random state within a bounded rectangular area centered on the AUV state.

The aMCL algorithm is called at each time step of the AUV controller, and carries out two main steps. The first step, often called *prediction*, randomly propagates all particle states according to stochastic motion model that simulates shark motion [25].

The second step, often called *correction*, is only called when a valid tag transmission is re-

ceived by the AUV. In this case the weight w_i for each particle $p_i \in P_t$ is calculated according to the sensor model in Eq. 8. Each particle has a minimum weight $w_{\text{min}} = 10^{-7}$. This model assigns higher weights when both the actual angle z_α measurements and calculated distance d match well with the particle's expected angle α_{exp} and distance d_{exp}. These expected values are calculated based on the geometry of the AUV state and particle's shark state.

$$w_i = w_{\text{min}} + \frac{1}{\sqrt{2\pi}\sigma_\alpha} e^{\frac{-(\alpha_{exp}-z_\alpha)^2}{2\sigma_\alpha^2}} * \frac{1}{\sqrt{2\pi}\sigma_d} e^{\frac{-(d_{exp}-d)^2}{2\sigma_d^2}} \tag{8}$$

After each particle is assigned a weight, the long- and short-term likelihoods of the sensor measurements, denoted by w_{slow} and w_{fast}, are calculated. From w_{slow} and w_{fast}, the probability p of adding random particles is calculated. The reader should consult Thrun et al. for the full details on how the probability p is calculated [24]. The correction steps shown in Alg. 2 then create a new set of particles P_{t+1}.

Algorithm 2 aMCL Correction Step

```
1:  for j = 1 to |P_t| do
2:      if p > Random(0,1) then
3:          add a random particle to P_{t+1}
4:      else
5:          choose p_i ∈ P_t with probability ∝ w_i
6:          add p_i to P_{t+1}
7:      end if
8:  end for
9:  if p < 0.5 then
10:     P ← P_{t+1}
11:     P_{t+1} ← {}
12:     re-calculate w_i for all p_i ∈ P
13:     for j = 1 to |P| do
14:         choose p_i ∈ P with probability ∝ w_i
15:         add p_i to P_{t+1}
16:     end for
17: end if
```

The addition of random particles in line 3 of Alg. 2 is the key step in preventing particle deprivation. The lines 9 to 16 in Alg. 2 are a modification to augmented MCL added by the authors. The particle weights are recalculated and a second re-sampling based on particle weights is done if $p < 0.5$. In simulation, the absence of lines 9 to 16 resulted in repeated cases of failure to recover from particle deprivation.

After both the prediction and correction steps are complete, the estimated shark state at time $t+1$ is calculated as the state averaged over all particles in P_{t+1}.

V. Experimental Results

A. Overview

Field testing was conducted at Big Fisherman Cove, at the Philip K. Wrigley Marine Science Center on Catalina Island. First, results comparing calculated time-of-flight distance and actual distance are presented. Next, the accumulation of random errors in calculated distance is examined. Third, results from active tracking of a tagged boat are presented. Finally, the effect of incorporating both distance and angle measurements in state estimation is examined.

B. Time of Flight Distance

Two sets of experiments benchmarking the accuracy of time-of-flight distance were conducted using Tag 55488. Since the tag was power cycled after the initial calibration of T_c and t_0, the initial time of transmission t_0 was recalibrated using Eq. 4. The first experiment was conducted on July 13, 2013 from 10:25 to 14:18. The tag was hung from the dock side and the absolute position of the tag was obtained by holding the AUV adjacent to the tag and recording its GPS measurements. The AUV was then tied to an anchored buoy approximately 85 m away from the tag. Approximately every 80 min, the AUV was untied and manually driven in a single loop between the dock and buoy before being retied to the buoy. Using the logged time-of-arrival of transmitted tag codes, the time-of-flight distances were calculated offline.

The second experiment was conducted on July 14, 2013 from 22:44 to 23:23, and included active tracking of tagged boat. Time-of-flight distance

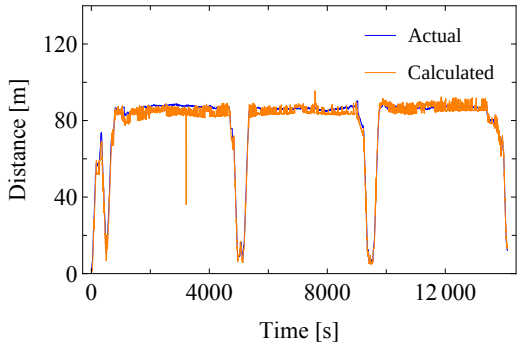

Fig. 4: Comparison of calculated distance against actual distance of the AUV from the tag.

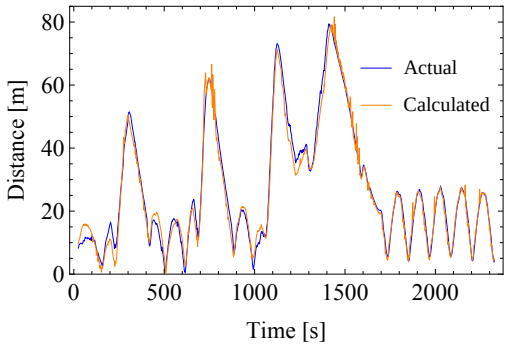

Fig. 5: Comparison of calculated distance against actual distance of the AUV from the tag during active tracking of a tagged boat.

was calculated online. Comparisons of the time-of-flight distance to actual distance are shown in Fig. 4 and Fig. 5, and their errors are summarized in Table III. Over these short time intervals, only several hours after calibration of t_0, the distance-to-tag errors remain on the order of only a few meters.

Experiment	Mean Error [m]	σ Error [m]
Tied to buoy	1.93	2.34
Active tracking	0.62	2.63

TABLE III: Errors in calculated time-of-flight distance of AUV from tag. Error is defined as the actual distance subtracted by calculated distance.

C. Accumulation of Random Error

Since the distance calculations rely on linear extrapolation from an initial transmission time t_0 and period T_c, the rate at which random errors in the distance accumulate was also examined. Tag 55436 was attached to a hydrophone for roughly 22 hours, during which the time-of-flight distances were calculated. The experiment results are shown in Fig. 6. Many factors could contribute in the

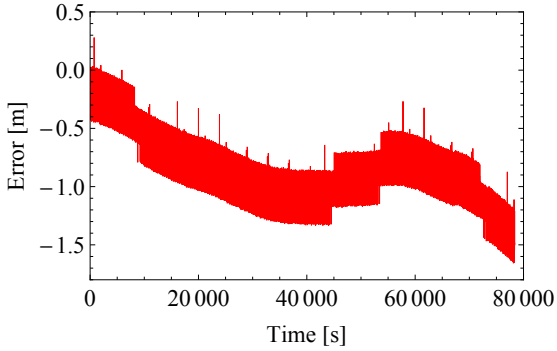

Fig. 6: Error of the calculated distance from the expected distance of 0 m, using the approximation of 1500 ms^{-1} for the speed of sound in seawater.

accumulation of the random errors. The battery level of the tag, power cycling the tag, and the length of the time interval used to calibrate T_c are all potential factors. In Fig. 6, an error of -1.5 m was observed after 22 hrs. However, in an identical experiment conducted on a different day, an error of 8 m was accumulated by the end of the experiment. To better understand the accumulation of random errors, this experiment should be repeated multiple times for multiple tags spanning their battery lives.

D. Online State Estimation

Active tracking of a tagged boat was conducted on July 14, 2013 from 22:44 to 23:23. The boat idled in an area for several minutes before relocating. This process was repeated multiple times. The position of the boat was logged using the GPS receiver on a Vemco VR100. The AUV's state estimator incorporated both distance and angle measurements to estimate tag position. Results

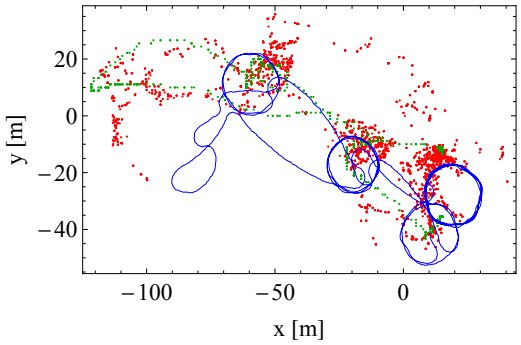

Fig. 7: Online localization and tracking of a tagged boat using distance and angle measurements. The AUV's path is shown by the blue line, and positions of the tagged boat are shown by the green dots. The red dots represent the estimated boat location.

are shown in Fig. 7. The associated localization error is plotted as a function of time in Fig. 8. Here localization error is defined as the distance between the actual boat position and the position estimated by the online state estimator.

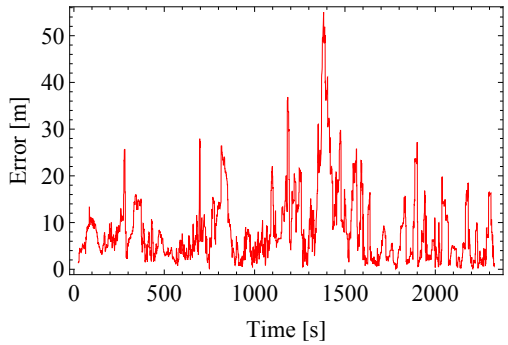

Fig. 8: Localization errors of a tagged boat as a function of time. The mean error is 8.46 m with a standard deviation of 7.82 m.

The ability of the state estimator to recover from bad localization of the tagged boat is illustrated in Fig. 9. At time 1388 s depicted in Fig. 9 (a), the boat was being driven back to the dock and the state estimator had an error of 47.6 m. At time 1745 s depicted in Fig. 9 (b) the boat was stationary at the dock and the state estimator had successfully re-localized the boat with an estimation error of 2.95 m.

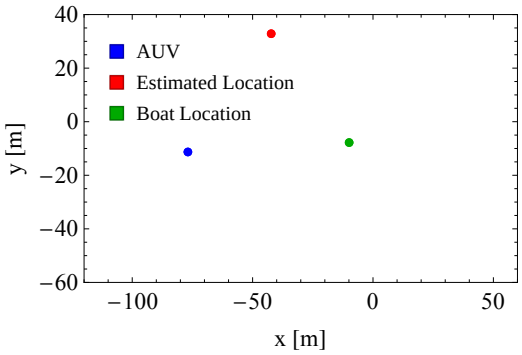

(a) The boat is being driven towards dock.

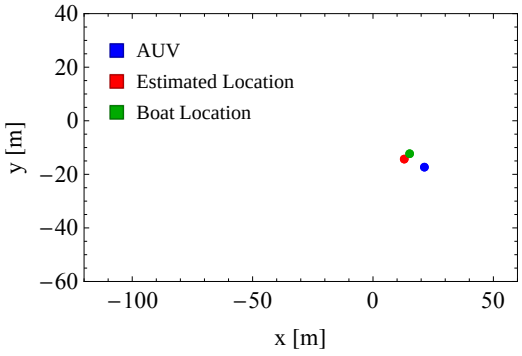

(b) The boat is now stationary at the dock.

Fig. 9: Two snap shots at two different showing the state estimator recovering from a bad state estimation. In (a), the estimation error is 47.6 m while the boat is being driven. In (b), the boat is successfully re-localized after it stopped at the dock.

E. Offline Comparison

To compare the effect of using distance measurements, state estimations were repeated offline using the recorded AUV states and the sensor measurements from the active tracking of the tagged boat. Offline state estimation using the following combinations of sensor measurements in the aMCL correction step were tested:

i. Only angle measurements
ii. Only distance measurements
iii. Both angle and distance measurements

For each combination of sensor measurements, the state estimator was run twenty times offline. The results are summarized in Table IV. Compared to using only angle, or only distance, using both angle and distance decreased the error in state estimation by a factor of two.

Measurements	Mean Error [m]	σ Error [m]
Angle	16.38	15.07
Distance	19.43	29.83
Angle and Distance	8.76	12.82

TABLE IV: Comparison of errors in offline state estimation using different measurement combinations.

The state estimation errors as a function of actual AUV distance-to-tag are summarized in Fig. 10. To evaluate the effect distance-to-tag had

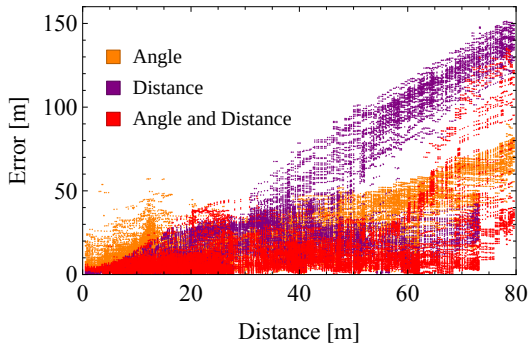

Fig. 10: Comparison of offline state estimation errors using different measurements as a function of actual distance of the AUV to the tagged boat.

on estimation error, the offline state estimation errors were grouped into three distance intervals: [0 m, 30 m), [30 m, 60 m), and [60 m, 90 m). The results are summarized in Fig. 11. In the short range interval [0 m, 30 m), errors were roughly the same regardless of the measurements used. In mid range interval [30 m, 60 m), estimation using both angle and distance performed best. In the long range interval [60 m, 90 m), estimation errors when using angle and distance measurements were generally lower. Even though the maximum error was higher, the 75^{th} percentile error from using both angle and distance measurements was the lowest within the longest range interval. Ideally,

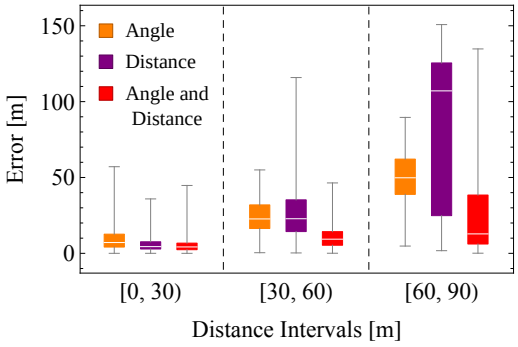

Fig. 11: Box and whisker plots showing offline state estimation errors at different AUV-to-tagged boat distance intervals.

the AUV will actively stay close to the target so as to minimize estimation errors associated with distance. In the unfortunate scenario where a large estimation error does occur, a compounding effect could occur where the AUV drives further from the target, thereby increasing the potential for even larger state estimation errors. Therefore, it is highly desirable that the estimation errors do not increase significantly as the distance to the tagged target increases.

VI. Conclusion

This paper presented a method of calculating distance from an AUV to an acoustic tag through the use of time-of-flight calculations. Experimental results showed that time-of-flight distance can be calculated with sufficient accuracy and precision to decrease errors in online state estimations of a tagged target by an AUV.

Despite the accumulating random errors in time-of-flight distance calculations, reliable distance measurements can still be obtained four hours after the calibration of the initial transmission time t_0.

Future work will include more extensive characterization of random errors in the distance calculations, such as examining the errors over longer periods of time and across a greater number of tags. Ideally this characterization will produce

methods for identifying and correcting such errors during online state estimation. The effect of incorporating distance measurements into state estimation will also be examined in a multi-AUV shark tracking system.

VII. Acknowledgment

This material is based upon work supported by the National Science Foundation under Grant No. 1245813. This work was performed in part at the Claremont Colleges' Robert J. Bernard Biological Field Station.

References

[1] M. Espinoza, T. J. Farrugia, D. M. Webber, F. Smith, and C. G. Lowe, "Testing a new acoustic telemetry technique to quantify long-term fine-scale movments of aquatic animals," *Fisheries Research*, vol. 108, pp. 364--371, 2011.

[2] C. G. Lowe and R. N. Bray, "Fish movement and activity patterns," *The Ecology of California Marine Fishes*, pp. 524--553, 2006.

[3] C. M. Clark, C. Forney, E. Manii, D. Shinzaki, C. Gage, M. Farris, C. Lowe, and M. Moline, "Tracking and following a tagged leopard shark with an autonomous underwater vehicle," *Journal of Field Robotics*, vol. 30, 2013.

[4] C. Forney, E. Manii, M. Farris, M. Moline, C. Lowe, and C. Clark, "Tracking of a tagged leopard shark with an auv: Sensor calibration and state estimation," in *Proceedings of the 4th International Conference on Robotics and Automation*, St. Paul, Minnesota, 2012.

[5] D. Schulz, W. Burgard, D. Fox, and A. Cramers, "Tracking multiple moving objects with a mobile robot," in *Computer Vision and Pattern Recognition, IEEE Computer Society Conference*, 2001.

[6] D. Schulz, W. Burgard, D. Fox, and A. Cremers, "People tracking with mobile robots using sample-based joint probabilistic data association filters," *The international Journal of Robotics Research*, vol. 22, 2003.

[7] M. Kobilarov, G. Sukhatme, J. Hyams, and P. Batavia, "People tracking and following with mobile robot using an omnidirectional camera and a laser," in *Proceedings of the 2006 IEEE International Conference on Robotics and Automation*, 2006.

[8] M. Montemerlo, S. Thrun, and W. Whittaker, "Conditional particle filters for simultaneous mobile robot localization and people-tracking," in *Proceedings of the 2002 IEEE International Conference on Robotics and Automation*, vol. 1, 2002, pp. 695--701.

[9] J. Rife and S. M. Rock, "Segmentation methods for visual tracking of deep-ocean jellyfish using a conventional camera," *IEEE Journal of Ocean Engineering*, vol. 28, pp. 595--608, 2003.

[10] T. Grothues, J. Dobarro, and J. Eiler, "Collecting, interpreting, and merging fish telemetry data from an auv: Remote sensing from an already remote platform," in *Authonomous Underwater Vehicles (AUV), 2010 IEEE/OES*, Monterey, CA, 2010, pp. 1--9.

[11] J. Rife and S. M. Rock, "Segmentation Methods for Visual Tracking of Deep-Ocean Jellyfish using a Conventional Camera," *IEEE Journal of Oceanic Engineering*, vol. 28, no. 4, pp. 595--608, 2003.

[12] J. Zhou and C. M. Clark, "Autonomous fish tracking by ROV using monocular camera," *Computer and Robot Vision, Canadian Conference*, vol. 0, p. 68, 2006.

[13] C. Georgiades, A. German, A. Hogue, H. Liu, C. Prahacs, A. Ripsman, R. Sim, L. Torres, P. Zhang, M. Buehler *et al.*, "Aqua: an aquatic walking robot," in *Intelligent Robots and Systems, 2004.(IROS 2004). Proceedings. 2004 IEEE/RSJ International Conference on*, vol. 4. IEEE, 2004, pp. 3525--3531.

[14] T. M. Grothues, J. Dobarro, J. Ladd, A. Higgs, G. Niezgoda, and D. Miller, "Use of a multi-sensored auv to telemeter tagged atlantic sturgeon and map their spawning habitat in the hudson river, usa," in *Autonomous Underwater Vehicles*, Woods Hole, MA, 2008, pp. 1--7.

[15] M. J. Oliver, M. W. Breece, D. A. Fox, D. E. Haulsee, J. T. Kohut, J. Manderson, and T. Savoy, "Shrinking the haystack: using and auv in an integrated ocean observatory to map atlantic sturgeon in the coastal ocean," *Fisheries*, vol. 38, 2013.

[16] T. Grothues and J. Dobarro, "Fish telemetry and positioning from an autonomous underwater vehicle (AUV)," *Instrumentation ViewPoint*, no. 8, p. 78, 2009.

[17] N. Kussat, C. Chadwell, and R. Zimmerman, "Absolute positioning of an autonomous underwater vehicle using gps and acoustic measurements," *IEEE Journal of Oceanic Engineering*, vol. 30, pp. 153--164, 2005.

[18] S. Thrun, D. Fox, W. Burgard, and F. Dellaert, "Robust Monte Carlo localization for mobile robots," *Artificial Intelligence*, vol. 128, no. 1-2, pp. 99--141, 2001.

[19] D. Fox, S. Thrun, W. Burgard, and F. Dellaert, "Particle filters for mobile robot localization," 2001.

[20] F. Gustafsson, F. Gunnarsson, N. Bergman, U. Forssell, J. Jansson, R. Karlsson, and P. Nordlund, "Particle filters for positioning, navigation, and tracking," *IEEE Transactions on Signal Processing*, vol. 50, no. 2, pp. 425--437, 2002.

[21] D. Fox, W. Burgard, F. Dellaert, and S. Thrun, "Monte Carlo localization: Efficient position estimation for mobile robots," in *Proceedings of the National Conference on Artificial Intelligence*. JOHN WILEY & SONS LTD, 1999, pp. 343--349.

[22] S. Thrun, "Particle filters in robotics," in *Proceedings of the 17th Annual Conference on Uncertainty in AI (UAI)*, vol. 1. Citeseer, 2002.

[23] S. Park, J. Hwang, K. Rou, and E. Kim, "A new particle filter inspired by biological evolution: Gentic filter," *World Academy of Science, Engineering and Technology*, vol. 33, 2007.

[24] S. Thrun, W. Burgard, and D. Fox, "Probabilis-

tic robotics," in *Probabilistic Robotics (Intelligent Robotics and Autonomous Agents)*. USA: The MIT Press, sept. 2005.

[25] D. Shinzaki, C. Gage, S. Tang, M. Moline, B. Wolfe, C. Lowe, and C. Clark, "A multi-auv system for cooperative tracking and following of leopard sharks," in *Proceedings of the IEEE International Conference on Robotics and Automation*, 2013.